9-26-2022

Capsaicin Inhibits Multiple Voltage-Gated Ion Channels in Rabbit Ventricular Cardiomyocytes in TRPV1-Independent Manner

Dmytro Isaev
Bogomoletz Institute of Physiology

Keun-Hang Susan Yang
Chapman University, kyang@chapman.edu

Waheed Shabbir
Bogomoletz Institute of Physiology

Frank Christopher Howarth
UAE University, Al Ain, Abu Dhabi, UAE

Murat Oz
Kuwait University, murat.oz@hsc.edu.kw

Recommended Citation

Isaev, D.; Yang, K.-H.S.; Shabbir, W.; Howarth, F.C.; Oz, M. Capsaicin Inhibits Multiple Voltage-Gated Ion Channels in Rabbit Ventricular Cardiomyocytes in TRPV1-Independent Manner. *Pharmaceuticals* 2022, https://doi.org/10.3390/ph15101187

Capsaicin Inhibits Multiple Voltage-Gated Ion Channels in Rabbit Ventricular Cardiomyocytes in TRPV1-Independent Manner

pharmaceuticals

MDPI

Article

Capsaicin Inhibits Multiple Voltage-Gated Ion Channels in Rabbit Ventricular Cardiomyocytes in TRPV1-Independent Manner

Dmytro Isaev [1], Keun-Hang Susan Yang [2], Waheed Shabbir [1], Frank Christopher Howarth [3] and Murat Oz [4,*]

[1] Department of Cellular Membranology, Bogomoletz Institute of Physiology, 01024 Kiev, Ukraine
[2] Department of Biological Sciences, Schmid College of Science and Technology, Chapman University, One University Drive, Orange, CA 92866, USA
[3] Department of Physiology, College of Medicine and Health Sciences, UAE University, Abu Dhabi 15551, United Arab Emirates
[4] Department of Pharmacology and Therapeutics, Faculty of Pharmacy, Kuwait University, Safat 13110, Kuwait
* Correspondence: ahmet.oz@ku.edu.kw; Tel.: +965-99758003

Abstract: Capsaicin is a naturally occurring alkaloid derived from chili pepper which is responsible for its hot, pungent taste. It exerts multiple pharmacological actions, including pain-relieving, anti-cancer, anti-inflammatory, anti-obesity, and antioxidant effects. Previous studies have shown that capsaicin significantly affects the contractility and automaticity of the heart and alters cardiovascular functions. In this study, the effects of capsaicin were investigated on voltage-gated ion currents in rabbit ventricular myocytes. Capsaicin inhibited rapidly activated (I_{Kr}) and slowly activated (I_{Ks}) K^+ currents and transient outward (I_{to}) K^+ current with IC_{50} values of 3.4 μM,14.7 μM, and 9.6 μM, respectively. In addition, capsaicin, at higher concentrations, suppressed voltage-gated Na^+ and Ca^{2+} currents and inward rectifier I_{K1} current with IC_{50} values of 42.7 μM, 34.9 μM, and 38.8 μM, respectively. Capsaicin inhibitions of I_{Na}, $I_{L\text{-}Ca}$, I_{Kr}, I_{Ks}, I_{to}, and I_{K1} were not reversed in the presence of capsazepine (3 μM), a TRPV1 antagonist. The inhibitory effects of capsaicin on these currents developed gradually, reaching steady-state levels within 3 to 6 min, and the recoveries were usually incomplete during washout. In concentration-inhibition curves, apparent Hill coefficients higher than unity suggested multiple interaction sites of capsaicin on these channels. Collectively, these findings indicate that capsaicin affects cardiac electrophysiology by acting on a diverse range of ion channels and suggest that caution should be exercised when capsaicin is administered to carriers of cardiac channelopathies or to individuals with arrhythmia-prone conditions, such as ischemic heart diseases.

Keywords: capsaicin; ion channels; rabbit; cardiomyocytes

Citation: Isaev, D.; Yang, K.-H.S.; Shabbir, W.; Howarth, F.C.; Oz, M. Capsaicin Inhibits Multiple Voltage-Gated Ion Channels in Rabbit Ventricular Cardiomyocytes in TRPV1-Independent Manner. *Pharmaceuticals* **2022**, *15*, 1187. https://doi.org/10.3390/ph15101187

Academic Editor: Gary J. Stephens

Received: 12 August 2022
Accepted: 20 September 2022
Published: 26 September 2022

1. Introduction

Capsaicin (8-methyl-N-vanillyl-6-nonenamide), as an algogen and prototypical activator of transient receptor potential vanilloid type 1 (TRPV1) channels, has been used extensively in pain research. In addition, capsaicin has been shown to play functional roles in a wide range of pathophysiological conditions, ranging from cardiovascular to respiratory and urinary diseases [1,2]. The effects of capsaicin on the cardiovascular system have been known for several decades. Activation of TRPV1 channels on capsaicin-sensitive sensory nerves in the cardiovascular system has been shown to release various neuropeptides and play important roles in physiological regulation, as well as the pathophysiology of cardiovascular diseases such as heart failure, myocardial infarction, and hypertension [3,4]. The vascular effects of capsaicin and the role of TRPV1 channels in the pathophysiology of hypertension is a complex process involving the TRPV1-dependent and independent action of capsaicin on the vascular endothelium, smooth muscle myocytes, and the peripheral and central nervous system, which have been reviewed in earlier studies [3,5–7].

In earlier studies, capsaicin has been shown to exert transient positive inotropic and chronotropic effects [8–10], which are reversed by TRPV1 antagonists such as ruthenium-

red [11,12] and capsazepine [12] and by the desensitization of TRPV1 [13,14] in isolated guinea-pig and rat atria. In vitro studies have demonstrated that positive inotropic and chronotropic effects of capsaicin (0.1–1 μM) are mediated by neuropeptides such as calcitonin gene-related peptide, neurokinin A, and vasoactive intestinal polypeptide released from capsaicin-sensitive-sensory neurons in guinea-pig- and rat-isolated atrial preparations [11,12,14–16].

Although previous studies have established a functional role of TRPV1 channels in mediating the positive inotropic and chronotropic effects of capsaicin, mainly in atrial preparations, the capsaicin-induced suppression of cardiac contractions and alterations in electrophysiological characteristics of action potentials have also been reported in ventricular papillary muscle and [10,17], whole-heart preparations [11,16,18,19], suggesting that capsaicin, in addition to TRPV1-mediated effects, exerts direct actions on the cardiac muscle. Thus, this study investigated the effects of capsaicin on major inward (Na^+ and Ca^{2+}) and outward (K^+) currents in rabbit ventricular myocytes, which are physiologically the most relevant cells to investigate the cellular and molecular targets of capsaicin actions observed in earlier studies in atrial and ventricular preparations.

2. Results

2.1. The Effects of Capsaicin on Na^+ Channels (I_{Na})

Inward I_{Na} was elicited by step depolarizations from a holding potential of −100 mV to −20 mV at 30 s intervals. The effects of 6 min capsaicin (30 μM) application and 8 min recovery on superimposed traces of I_{Na} are shown in Figure 1A. The bath application of capsaicin caused a gradually progressing suppression of I_{Na}, which reached steady-state levels within 4–5 min (Figure 1B). The recovery was partial during the experiments lasting up to 15 to 18 min. The current–voltage (*I-V*) relationship for I_{Na} is presented in Figure 1C. No significant changes in the *I-V* relationship were observed; the threshold, peak, and reversal potentials for I_{Na} remained unaltered (n = 5). The extent of the capsaicin suppression of I_{Na} was not altered by changes in the test potentials (Figure 1D). The concentration-dependency of capsaicin inhibition is presented in Figure 1E. The IC_{50} value and apparent Hill coefficient were 42.7 μM and 1.4, respectively (n = 4–7). The bath application of capsazepine (3 μM) for 10 min did not alter the peak I_{Na} (n = 4). The extent of capsaicin inhibition of I_{Na} was not altered by the co-application of 3 μM capsazepine, an antagonist of the TRPV1 receptor, and 30 μM capsaicin (n = 6–7, $p > 0.05$; *t*-test).

2.2. The Effects of Capsaicin on L-Type Ca^{2+} Channels ($I_{L\text{-}Ca}$)

$I_{L\text{-}Ca}$ was studied in the presence of extracellular TEA^+ and intracellular Cs^+ to suppress K^+ currents. In addition, the contaminating Na^+ current was eliminated by applying test potentials from a relatively depolarized potential of −50 mV to induce the inactivation of I_{Na} [20]. The superimposed traces of the currents elicited by the test potentials from −50 mV to +20 mV in the control, after a 5 min application of 30 μM capsaicin and 7 min recovery, are shown in Figure 2A. The bath application of capsaicin caused a steadily progressing inhibition of $I_{L\text{-}Ca}$, which was detectable within 30 sec and reached a steady-state level within 3–5 min, and the recovery was partial (Figure 2B). The *I-V* relationships in the control and in the presence of 30 μM capsaicin are presented in Figure 2C (n = 5). The relationship between the test potentials and the extent of capsaicin inhibition of $I_{L\text{-}Ca}$ was presented in Figure 2D (n = 5). Capsaicin inhibited $I_{L\text{-}Ca}$ in a concentration-dependent manner with an IC_{50} value of 34.9 μM and an apparent Hill coefficient of 1.3 (n = 3–6; Figure 2E). The application of capsazepine (3 μM) for 10 min did not affect the peak I_{Na} (n = 4). The extent of capsaicin inhibition of I_{Na} was not altered by the co-application of 3 μM capsazepine, an antagonist of the TRPV1 receptor, and 30 μM capsaicin (n = 5–7, $p > 0.05$; *t*-test).

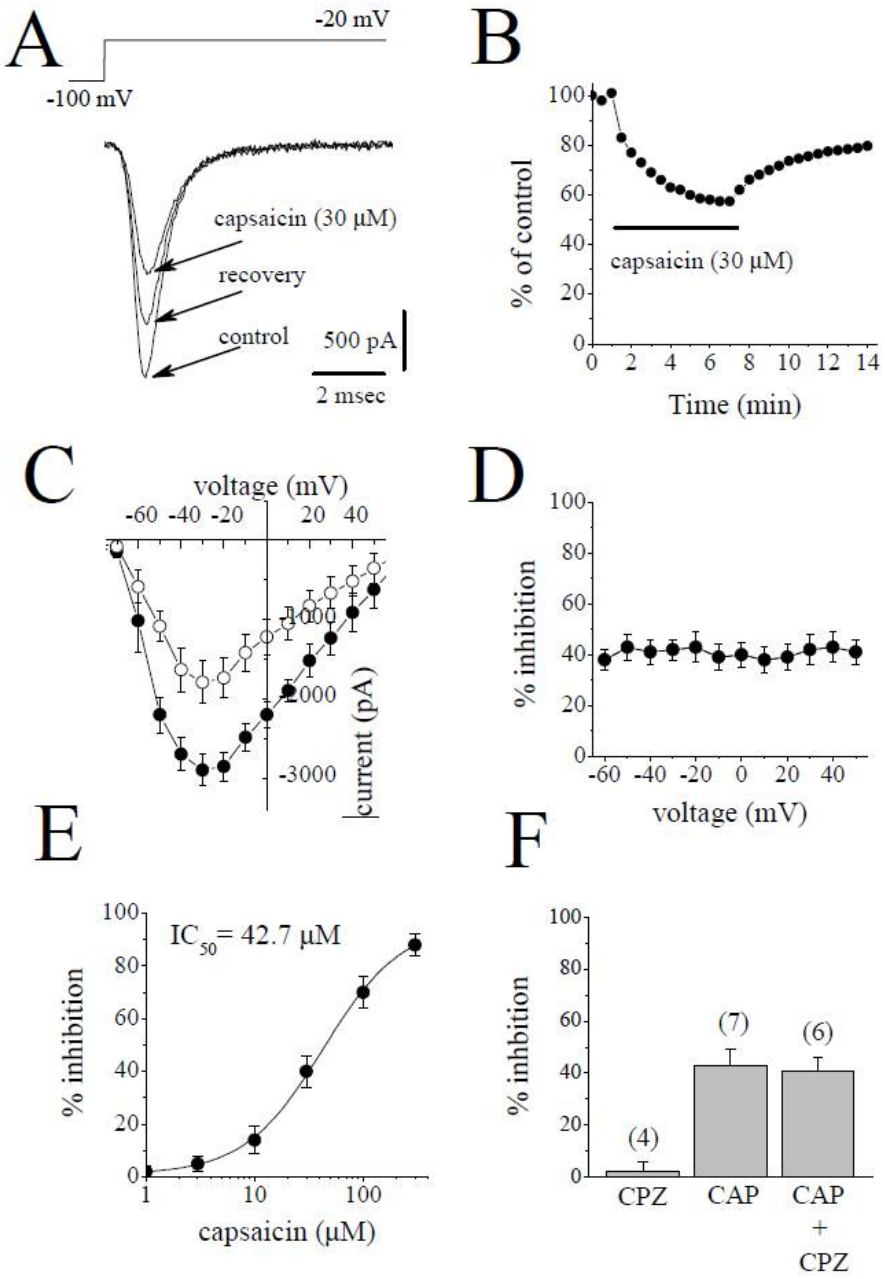

Figure 1. Capsaicin inhibits I_{Na} in rabbit ventricular myocytes. (**A**) Superimposed current traces in control conditions, 6 min after exposure to 30 μM capsaicin, and 8 min recovery. The pulse protocol to activate I_{Na} is shown as in inset. (**B**) Time course of the effect of capsaicin on the maximal amplitudes of I_{Na} as % of control current calculated as the mean of three consecutive control currents at the beginning of the experiment. (**C**) Current–voltage relationship of I_{Na} in the absence and presence of 30 μM capsaicin are presented with filled and open circles, respectively (n = 5). (**D**) Relationship between the extent of capsaicin (30 μM) inhibition of I_{Na} and test potential (n = 5; $p > 0.05$, ANOVA). (**E**) Concentration-inhibition curve for capsaicin inhibition of I_{Na} (n = 4–7). (**F**) The effect of capsazepine (3 μM) and the extent of capsaicin (30 μM) inhibition of I_{Na} in the absence and presence of 3 μM capsazepine. The number of cells tested for each group was presented on top of each bar ($p > 0.05$; t-test).

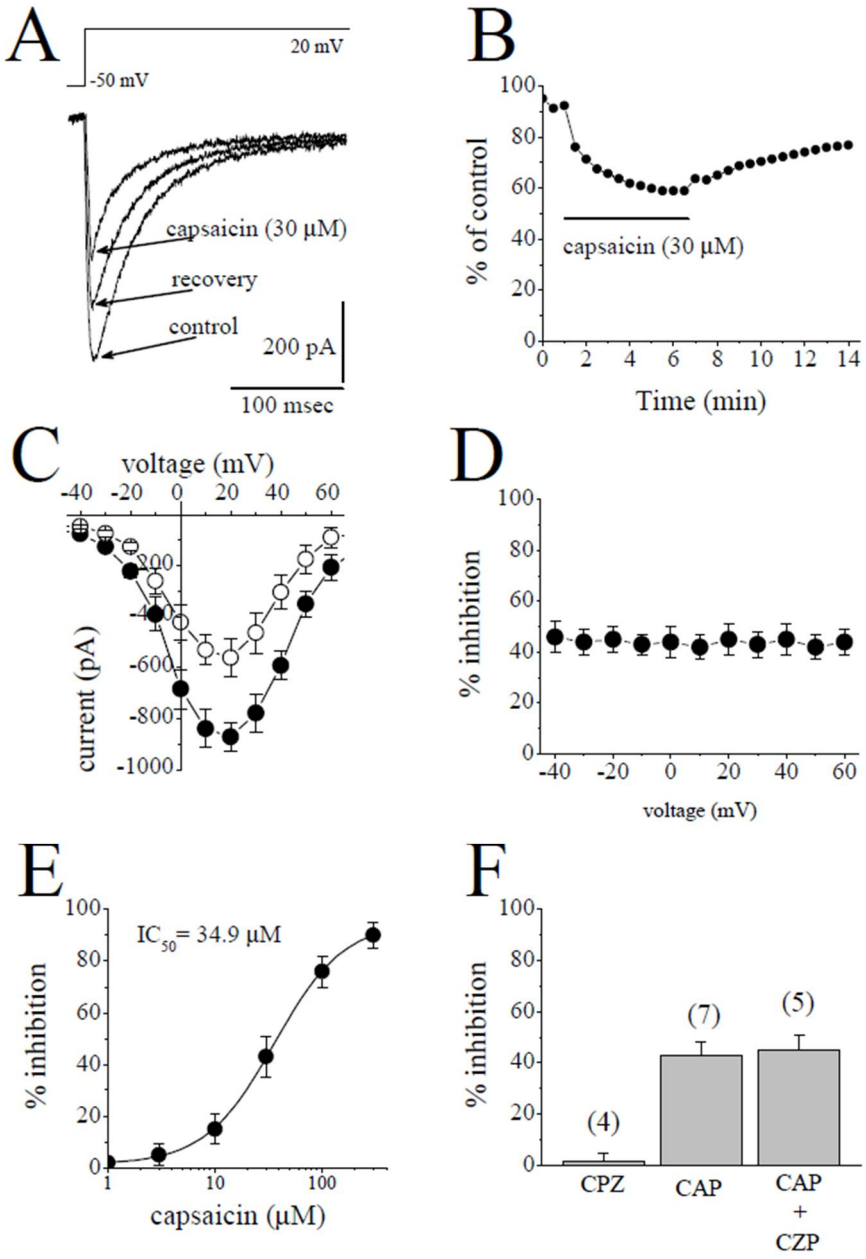

Figure 2. Capsaicin suppresses the $I_{L\text{-}Ca}$ in rabbit ventricular myocytes. (**A**) Superimposed current traces in control, after 5 min exposure to 30 μM capsaicin and recovery. The pulse protocol to evoke $I_{L\text{-}Ca}$ is shown as an inset. (**B**) Time course of the effect of capsaicin on the maximal amplitudes of $I_{L\text{-}Ca}$ presented as % of control calculated from the mean of three control currents. (**C**) Current–voltage curves of $I_{L\text{-}Ca}$ in the absence and presence of 30 μM capsaicin are presented with filled and open circles, respectively (n = 5). (**D**) The relationship between test potential and the capsaicin (30 μM) inhibition of $I_{L\text{-}Ca}$ (n = 5; $p > 0.05$, ANOVA). (**E**) Concentration-inhibition relationship for capsaicin suppression of $I_{L\text{-}Ca}$ (n = 3–6). (**F**) The effect of capsazepine (3 μM) and the extent of capsaicin (30 μM) inhibition of $I_{L\text{-}Ca}$ in the absence and presence of 3 μM capsazepine. The number of cells tested for each group was presented on top of each bar ($p > 0.05$; t-test).

2.3. The Effects of Capsaicin on the Delayed Rectifier K^+ Channels (I_K)

The delayed rectifier K^+ current in mammalian ventricular myocytes consists of a rapidly activating but inwardly rectifying I_{Kr} and a slowly activating I_{Ks} [21,22].

Rapidly activating delayed rectifier (I_{Kr}) was quantified by applying a test pulse from −40 mV to +40 mV and measuring the deactivating tail currents in response to repolarizing

test pulse of −40 mV. The difference between the peak of the tail current and the current at the beginning of test potential was taken as an estimate of I_{Kr}. The contribution of I_{Ks} was suppressed by 3 μM of selective I_{Ks} blocker HMR 1556 to increase the proportion of I_{Kr}. Traces of tail currents elicited by test potentials from +40 mV to −40 mV are presented for control and after 6 min application of 10 μM capsaicin and 7 min recovery in Figure 3A. The bath application of 10 μM capsaicin caused the inhibition of I_{Kr}, which was evident at 30 sec and reached a steady-state level within 5 min, and recovery was almost complete within the time course of the experiment (Figure 3B). The effects of 3 μM capsaicin on the *I-V* relationship of I_{Kr} are presented in Figure 3C (n = 5). The extent of the capsaicin inhibition at test potentials ranging from −20 to 50 mV is shown in Figure 3D (n = 5).

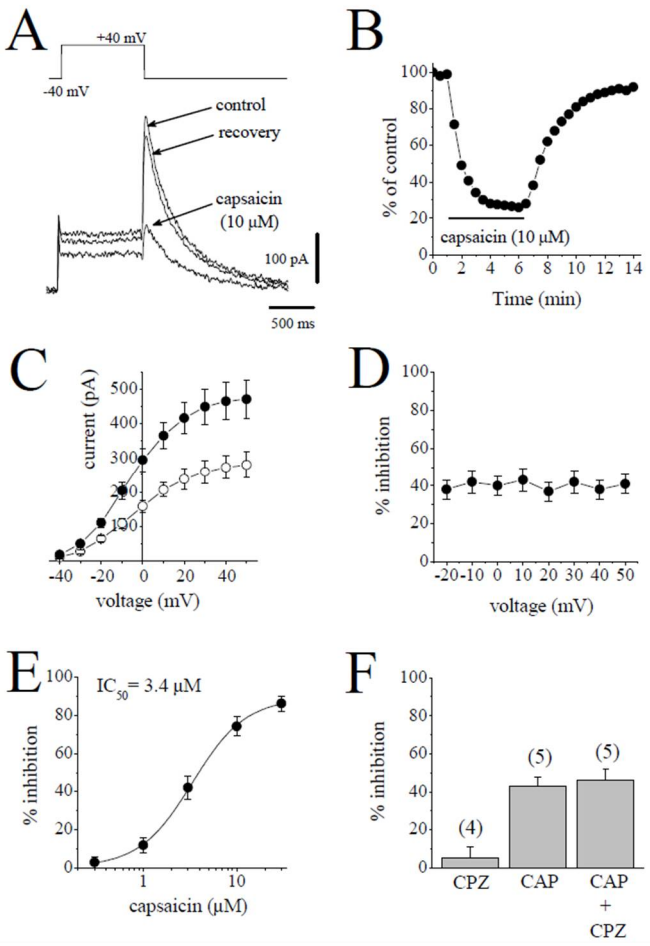

Figure 3. Capsaicin suppresses the I_{Kr} tail current. (**A**). Superimposed current traces in control, after 6 min exposure to 10 μM capsaicin and recovery. I_{Kr} tails were measured as a time-dependent component of the tail current activated in response to membrane repolarization. The pulse protocol to activate I_{Kr} is presented as an inset. (**B**) Time course of the effect of capsaicin effect on the maximal amplitudes of I_{Kr} and washout presented as % of control calculated from the mean of three control currents (n = 5). (**C**) Current–voltage relationships of I_{Kr} in absence (filled circles) and presence (open circles) of 3 μM capsaicin are shown (n = 6). (**D**) The relationship between test potential and the capsaicin (3 μM) inhibition of I_{Kr} (n = 6; $p > 0.05$, ANOVA). (**E**) Concentration-inhibition curve for capsaicin inhibition of I_{Kr} tails (n = 4–8). (**F**) The effect of capsazepine (3 μM) alone and the extent of capsaicin (3 μM) inhibition of I_{Kr} in the absence and presence of 3 μM capsazepine. The number of cells tested for each group was presented on top of each bar ($p > 0.05$; t-test).

The concentration-dependent effects of capsaicin are shown in Figure 3E. The IC_{50} value and apparent Hill coefficient were 3.4 μM and 1.4, respectively (n = 4–8). The bath application of 3 μM capsazepine did not affect the peak amplitudes of I_{Kr} tails (n = 4).

The extent of the capsaicin inhibition of I_{Kr} was not altered by the co-application of 3 μM capsazepine and capsaicin (3 μM) (Figure 3F; n = 5–6, $p > 0.05$).

Slowly activating delayed rectifier (I_{Ks}) was measured as the time-dependent current induced by 500 ms pulses from −50 to +60 mV. The superimposed current traces are shown for the control after an 8 min application of 10 μM capsaicin and a 5 min recovery in Figure 4A. The application of capsaicin caused a gradually developing inhibition of I_{Ks}, which reached a steady-state level within 6 min and recovered partially during the experiments (Figure 4B). Figure 4C shows the effect of 10 μM capsaicin on the *I-V* relationship of I_{Ks} (n = 5). The extent of capsaicin inhibition at test potentials ranging from −40 to 60 mV is shown in Figure 4D (n = 5). The concentration-dependent inhibition of I_{Ks} is presented in Figure 4E. The IC_{50} value and apparent Hill coefficient were 14.7 μM and 1.3, respectively (n = 4–6). The bath application of 3 μM capsazepine did not affect the peak amplitudes of I_{Ks} (n = 4). The extent of capsaicin inhibition of I_{Ks} was not altered by the co-application of 3 μM capsazepine and 3 μM capsaicin (Figure 4F; n = 5–6, $p > 0.05$).

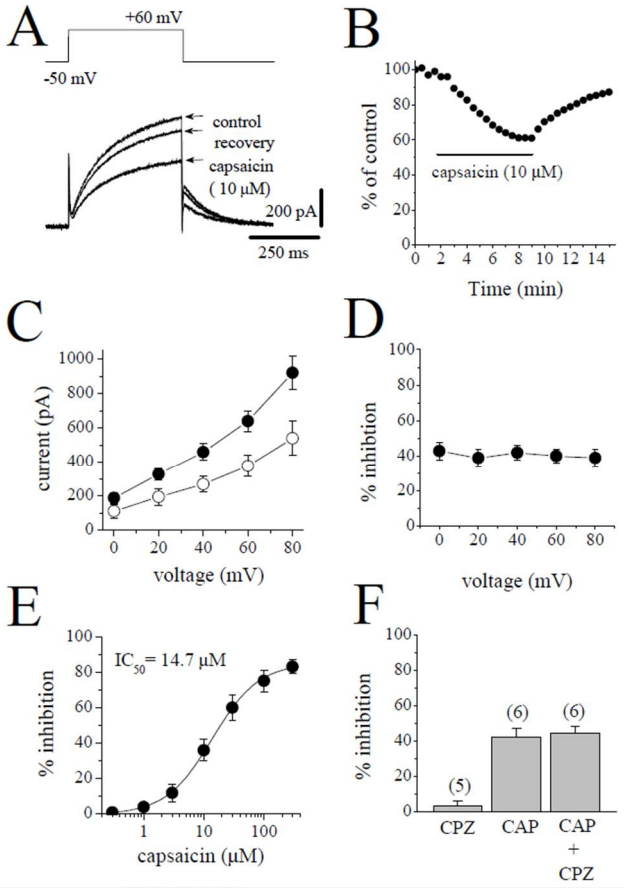

Figure 4. Capsaicin suppresses the I_{Ks} component of the delayed rectifying I_K. (**A**) Superimposed current traces in control, after 8 min exposure to 10 μM capsaicin, and recovery. The pulse protocol to activate I_{Ks} is shown as an inset. (**B**) Time course of the effect of capsaicin effect on the maximal amplitudes of I_{Ks} and washout presented as % of control calculated from the mean of three control currents. (**C**) Current–voltage relationships of I_{Ks} in the absence and presence of 10 μM capsaicin are presented with filled and open circles, respectively (n = 5). (**D**) The relationship between test potential and the capsaicin (10 μM) inhibition of I_{Ks} (n = 5; $p > 0.05$, ANOVA). (**E**) Concentration-inhibition curve for capsaicin inhibition of I_{Ks} (n = 4–6). (**F**) The effect of capsazepine (3 μM) and the extent of capsaicin (10 μM) inhibition of I_{Ks} in the absence and presence of 3 μM capsazepine. The number of cells tested for each group was presented on top of each bar ($p > 0.05$; t-test).

2.4. The Effect of Capsaicin on Transient Outward K^+ Current (I_{to})

I_{to} was activated by 400 ms test pulses from −80 mV to +60 applied at 30 s intervals and defined as the difference between the initial transient peak of the current and the maintained current at the end of the pulse. The superimposed current traces in the absence and 6 min presence of 10 μM capsaicin and during an 8 min recovery are presented in Figure 5A. The time course of the effect of bath application of capsaicin on the peak amplitudes of I_{to} is shown in Figure 5B. The *I-V* relationships of I_{to} in the absence and presence of 10 μM capsaicin are shown in Figure 5C (n = 7). The relationship between the test potentials and the extent of the capsaicin inhibition of I_{to} was presented in Figure 5D (n = 7). Figure 5E shows the concentration–inhibition curve of capsaicin on I_{to} (n = 4–7 cells). The IC_{50} and apparent Hill coefficient were 9.6 μM and 1.4, respectively. Capsazepine (3 μM) alone did not affect the peak amplitudes of I_{to} (n = 4). The extent of capsaicin inhibition of I_{to} was not altered by the co-application of 3 μM capsazepine and 10 μM capsaicin (Figure 5F; $p > 0.05$ *t*-test).

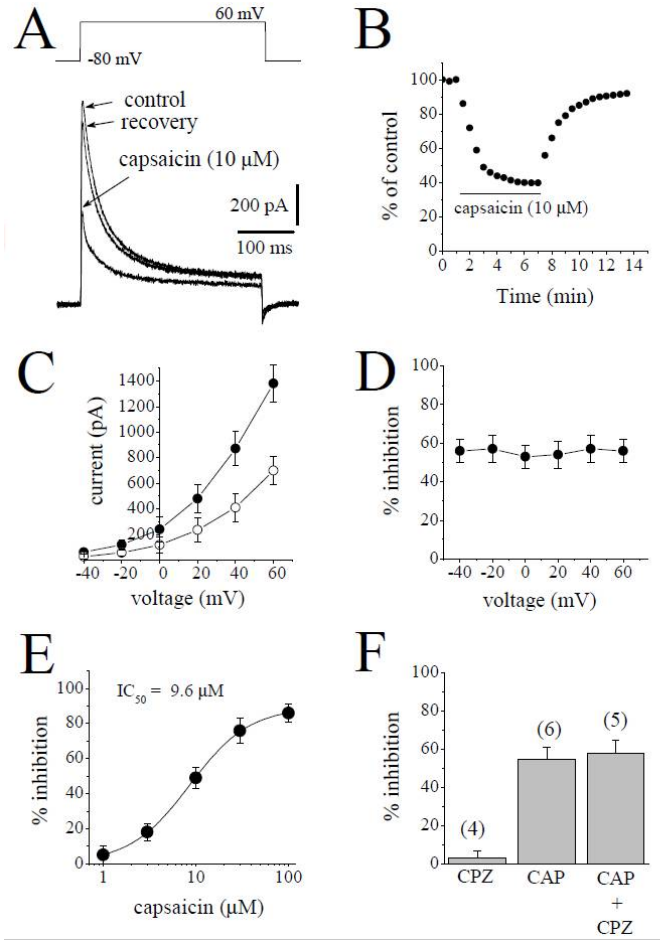

Figure 5. The effects of capsaicin on the transient outward I_{to} in rabbit ventricular myocytes. (**A**) Traces of I_{to} obtained in response to depolarizations from a holding potential of −80 mV to +60 mV are presented in control after 6 min exposure to 10 μM capsaicin and recovery. The pulse protocol to activate I_{to} is presented as an inset. (**B**) Time course of the effect of capsaicin effect on the maximal amplitudes of I_{to} and washout presented as % of control calculated from the mean of three control currents. (**C**) Current–voltage relationships of I_{to} in absence (filled circles) and presence (open circles) of 10 μM capsaicin are shown (n = 5). (**D**) The relationship between test potential and the capsaicin (10 μM) inhibition of I_{to} (n = 5; $p > 0.05$, ANOVA). (**E**) Concentration–inhibition of capsaicin for I_{to} (n = 4–7). (**F**) The effect of capsazepine (3 μM) and the extent of capsaicin (10 μM) inhibition of I_{to} in the absence and presence of 3 μM capsazepine. The number of cells tested for each group was presented on top of each bar ($p > 0.05$; *t*-test).

2.5. The Effect of Capsaicin on the Inward Rectifier K^+ Current (I_{K1})

I_{K1} was activated from the holding potential of −80 mV to the test potential of −120 mV. The amplitude of I_{K1} was determined by measuring the peak current relative to zero current. The traces of the currents in the control, in the presence of 30 μM capsaicin, and during recovery are shown in Figure 6A. Figure 6B shows the time course of the capsaicin effect and washout on I_{K1}. The *I-V* relationships of I_{K1} in the absence and presence of 30 μM capsaicin are presented in Figure 6C (n = 5). The relationship between the test potentials and the extent of the capsaicin inhibition of I_{K1} is presented in Figure 6D (n = 5). Figure 6E demonstrates the concentration–inhibition curve of capsaicin on I_{K1} (n = 4–6 cells). The IC_{50} and apparent Hill coefficient were 38.8 μM and 1.4, respectively. Capsazepine (3 μM) alone did not affect the peak amplitudes of I_{K1}. The extent of capsaicin inhibition of I_{K1} was not altered by the co-application of 3 μM capsazepine and 10 μM capsaicin (Figure 6F; $p > 0.05$; *t*-test).

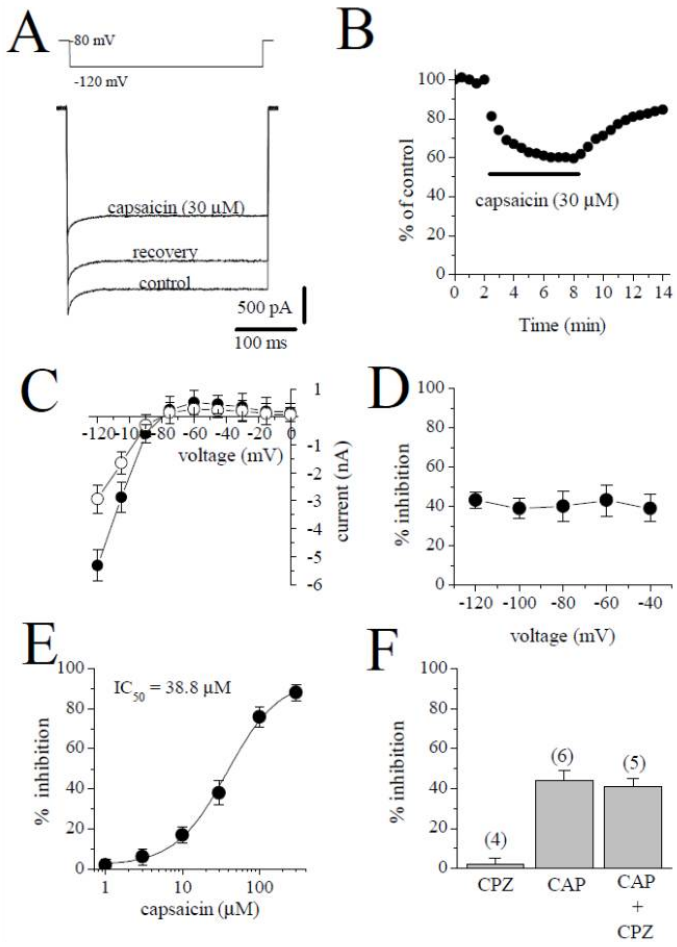

Figure 6. The effect of capsaicin on I_{K1}. (**A**) Traces of I_{K1} obtained in control after 6 min exposure to 30 μM capsaicin and recovery. The pulse protocol to activate I_{K1} is presented as an inset. (**B**) Time course of the effect of capsaicin effect on I_{K1} and washout presented as % of control calculated from the mean of three control currents. (**C**) Current–voltage relationships of I_{K1} in the absence and presence of 30 μM capsaicin were presented with filled and open circles, respectively (n = 5). (**D**) The relationship between test potential and the capsaicin (10 μM) inhibition of I_{K1} (n = 5; $p > 0.05$, ANOVA). (**E**) The effect of increasing concentration of capsaicin on I_{K1} (n = 4–6). (**F**) The effect of capsazepine (3 μM) and the extent of capsaicin (30 μM) inhibition of I_{K1} in the absence and presence of 3 μM capsazepine. The number of cells tested for each group was presented on top of each bar ($p > 0.05$; *t*-test).

3. Discussion

The results have demonstrated that capsaicin at concentrations higher than those required for the activation of TRPV1 channels directly inhibits the functions of multiple ion channels in rabbit ventricular myocytes. Capsaicin appears to effectively inhibit delayed rectifier K^+ currents (I_{Kr} and I_{Ks}) and I_{to}, with IC_{50} values of 3.4 μM,14.7 μM, and 9.6 μM, respectively. On the other hand, I_{Na}, $I_{L\text{-}Ca}$, and I_{K1} seem to be significantly less sensitive to capsaicin, with respective IC_{50} values of 42.7 μM, 34.9 μM, and 38.8 μM.

Although this is the first report on the capsaicin inhibition of I_{Kr} and I_{Ks}, in earlier studies, capsaicin was reported to inhibit I_{to}, and the I_{K1}, with IC_{50} values of 6.4 μM and 46.9 μM, respectively, in rat ventricular myocytes [23]. Similarly, the inhibition of I_{to} by capsaicin (IC_{50} = 5 μM) was reported in rat atrial myocytes [24]. In addition, capsaicin suppresses I_{HERG}, which corresponds to a rapid component of the delayed rectifier K^+ channel, expressed in *Xenopus* oocytes with an IC_{50} of 17.5 μM [25]. These results are in agreement with our findings on K^+ currents in rabbit ventricular myocytes.

Capsaicin, at significantly higher concentrations, suppressed I_{Na}, $I_{L\text{-}Ca}$, I_{K1} with IC_{50} values of 42.7 μM, 34.9 μM, and 38.8 μM, respectively. In an earlier study, capsaicin, at lower concentrations (0.4–4 μM), was reported to significantly suppress I_{Na} in rat atrial myocytes [26]. Similarly, capsaicin, at a significantly lower concentration of 0.33 μM, inhibited Vmax during phase 0 of action potential in guinea-pig papillary muscle [10]. However, other studies reported that capsaicin suppresses Vmax of action potentials in the concentration range of 30–120 μM in guinea-pig papillary muscle [27]. In a recent study, in agreement with our findings (IC_{50} = 42.7 μM), capsaicin inhibited cardiac Na^+ channels ($Na_V1.5$) with an IC_{50} of 60.2 μM in HEK-293 cells [28]. Although the present study is the first to report the inhibition (IC_{50} = 34.9 μM) of $I_{L\text{-}Ca}$ by capsaicin in cardiomyocytes, in agreement with our findings, capsaicin, at similar concentrations (10–30 μM) suppressed Vmax of Ca^{2+}-dependent action potentials in rabbit atrioventricular node [29] and sinoatrial cells [30].

The simulation with LabHEART, a computer model of rabbit ventricular action potentials [31], revealed that the suppression of I_{Ks}, I_{Kr}, and I_{to} at a concentration of 10 μM, capsaicin, as expected, causes a marked prolongation (39%) of action potential duration at 50% repolarization (APD_{50}), whereas the addition of the inhibition of I_{Na}, $I_{L\text{-}Ca}$, and I_{K1} at higher capsaicin concentration (30 μM) results in a 27% shortening of APD_{50} (Figure 7A). In earlier studies, capsaicin at concentrations higher than 1 μM has been reported to prolong APD in rat ventricular [23,24] and guinea-pig atrial [19] myocytes. On the other hand, capsaicin, at concentrations of 10 μM and higher, has been shown to decrease APD in guinea-pig papillary muscles [10,27,32] and canine cardiomyocytes for zucapsaicin [33]. Both the increase and decrease in APD can potentially have arrhythmogenic effects depending mainly on the underlying pathophysiological mechanisms, such as ischemic heart diseases. Our LabHEART simulation of rabbit ventricular myocytes also indicates that the high concentration of capsaicin (30 μM) can markedly depress intracellular Ca^{2+} transients (Figure 7B) and tension development (Figure 7C).

TRPV1 channels are not expressed in adult rat [34] and mouse [35,36] cardiomyocytes but may play roles at earlier developmental stages of myocytes [36,37]. In line with these findings, the effects of capsaicin on ion channels tested in this study (I_{Kr}, I_{Ks}, I_{to}) were not reversed by capsazepine, a TRPV1 antagonist. In addition, the bath application of capsaicin (1–30 μM), even at concentrations 10–100 times higher than those required to activate TRPVI channels, did not change the holding currents under patch-clamp conditions to record I_{Na} and $I_{L\text{-}Ca}$ (n = 14, data not shown), suggesting that TRPV1 is not involved in the observed effects of capsaicin. Cannabinoid receptors (CB1 and CB2) have been shown to be expressed in rat hearts [38], and capsaicin at concentrations higher than 10 μM was reported to bind to CB1 and CB2 receptors [39]. However, the co-application of specific CB1 antagonist SR141716A (2 μM) or specific CB2 antagonist SR 144528 (2 μM) and capsaicin did not alter the extent of the capsaicin inhibition of I_{Na} and $I_{L\text{-}Ca}$ (Paired t-test; $p > 0.05$;

n = 4–5), suggesting that CB1 and CB2 receptors are not involved in the capsaicin inhibition of these ion channels.

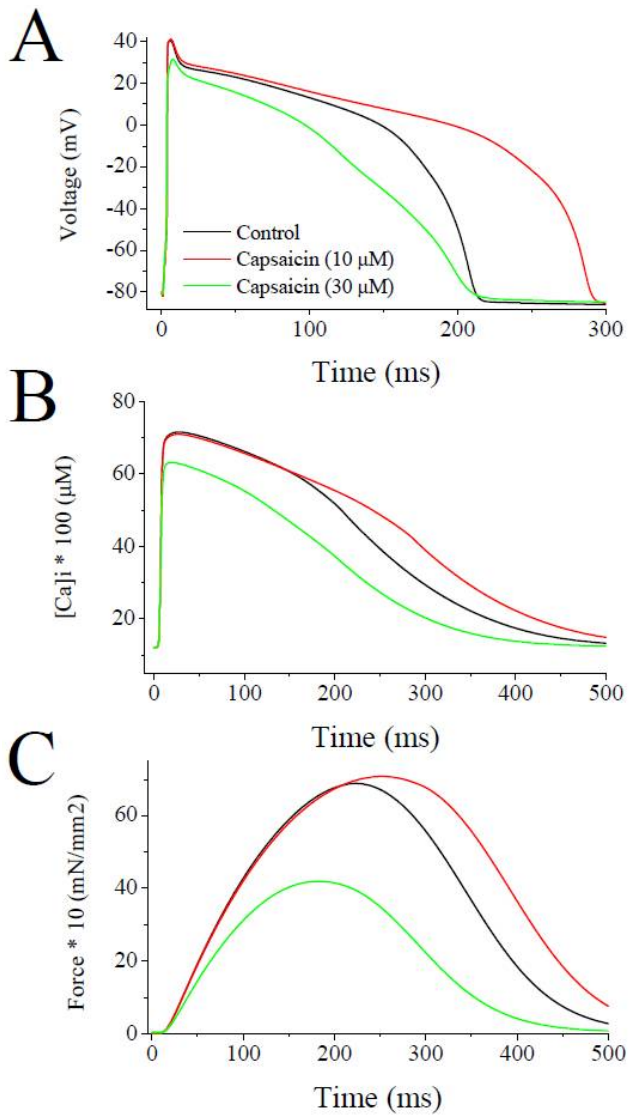

Figure 7. Effects of low and high concentrations of capsaicin on the simulated action potentials, intracellular Ca^{2+} transients, and force development during a single twitch response using LabHEART simulations. (**A**) At 10 μM capsaicin concentrations, the inhibition of I_{Kr}, I_{Ks}, I_{to} was incorporated. Whereas, at 30 μM capsaicin concentrations inhibitions of I_{Kr}, I_{Ks}, I_{to}, I_{K1}, I_{Na}, and $I_{Ca\text{-}L}$ were incorporated into the model. At 10 μM concentration, capsaicin induced marked prolongation (39%) of APD_{50}, while at higher concentration (30 μM) significantly shortened (27%) the APD_{50}. (**B**) Capsaicin, at the concentration of 10 μM, caused a slight delay in decay phase of Ca^{2+} transient. At higher concentration of 30 μM, capsaicin induced a marked suppression of Ca^{2+} transient. (**C**) Capsaicin, at 10 μM concentrations, caused a slight delay in decay phase of force development, but at higher concentrations of 30 μM, capsaicin induced a marked inhibition of force development during a simulated twitch response of a rabbit ventricular cardiomyocyte.

It is likely that capsaicin, a highly lipophilic agent with a LogP (octanol–water partition coefficient) value of 3.8, permeates the lipid membrane and then diffuses into the lipid membrane, and then alters the functional properties of the ion channels. Molecular dynamics simulations suggested that capsaicin is localized to the bilayer/solution interface [40]. Capsaicin was reported to regulate the functions of voltage-gated Na^+ and K^+ channels, as well as antibiotic-induced ion channels [41], by altering the biophysical properties of

the lipid membranes, such as the bilayer elasticity [40,42], dipole potential [43], and lipid disordering [44].

The effect of capsaicin on the ion channels tested in this study reached a maximal level within several minutes (3–6 min) of application. Similarly, the actions of several lipophilic modulators, including capsaicin [42,45,46], endocannabinoids [47–49], and general anesthetics [50,51] and steroids [52] on various ion channels require 5–15 min to reach their maxima with, in many cases, Hill coefficients of higher than unity in their concentration–effect curves, suggesting that the multiple binding sites for these allosteric modifiers are located inside the lipid membrane and require a relatively slow (in minutes) time course to reach equilibrium to modulate the functions of these channels. Thus, the accumulation of capsaicin in the lipid membrane appears to be a function of both the exposure time and concentration of capsaicin. Thus, while low capsaicin concentrations require longer exposure times, higher concentrations reach a threshold concentration at faster time scales to affect channel functions. In line with this assumption, the application of low concentrations (0.1–0.3 μM) for relatively long exposures (10–20 min) causes gradually developing suppression of contractility in guinea-pig papillary [10] and ventricular [19] muscle and whole heart [11] preparations. In another in vitro study, the 30 min administration of capsaicin, at concentrations as low as 1 nM, significantly inhibited the contractions of rat ventricular papillary muscle in a reversible manner [17]. In agreement with these findings, we have found that time to reach steady-state inhibition by capsaicin was inversely correlated with capsaicin concentrations applied to the ion currents investigated in this study (Figure 8). In addition to partitioning into the lipid bilayer and subsequently altering the biophysical characteristics of the plasma membrane, capsaicin can bind directly to ion channel domains embedded in cell membranes and affect the energy requirements for the gating-related conformational changes in ion channels [49].

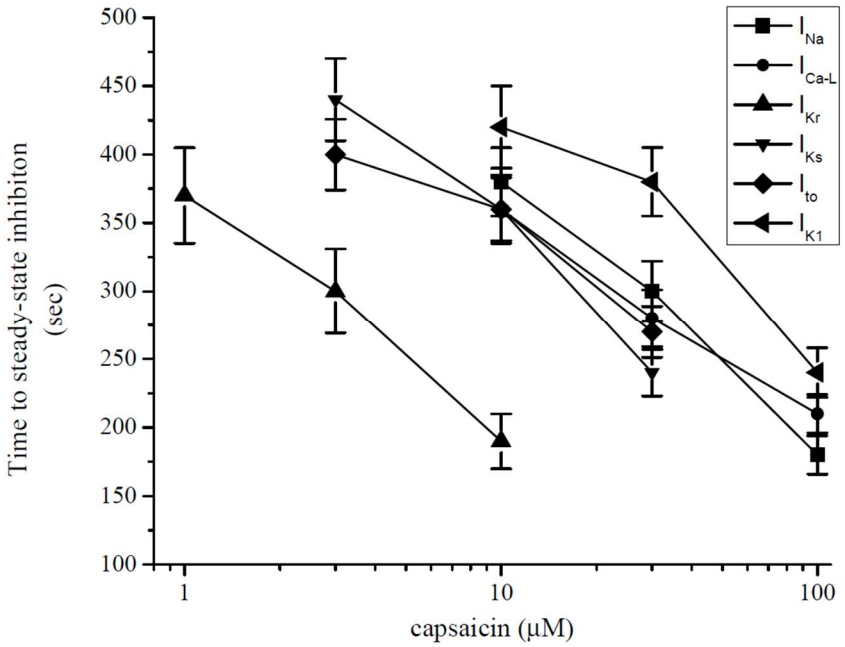

Figure 8. Relationship between time to reach steady-state maximal inhibition and capsaicin concentration for I_{Na}, $I_{L\text{-}Ca}$, I_{Kr}, I_{Ks}, I_{to}, and I_{K1} (each data point indicates mean ± SEM from 5–7 cells). Steady-state level was determined when three consecutive data points had the same (within the 97%) values.

In recent years, capsaicin has been administered as a dietary supplement for weight management and appetite suppression. Pharmacokinetic studies indicate that about 80% of ingested capsaicin is absorbed through the gastrointestinal system, leading to peak concentrations at sub-μM levels with a half-time of 30–60 min [1,53]. Thus, the regular

intake of low-dosage capsaicin supplements (1–30 mg/day) would not reach blood levels that would cause the significant inhibition of K^+ channels investigated in this study. However, as mentioned earlier, capsaicin is a highly lipophilic compound (LogP = 3.8), and its concentration in the cell membrane is expected to be considerably higher than blood levels. In animal studies, after intravenous or subcutaneous administrations, the capsaicin concentrations in the brain and spinal cord were found to be five-fold higher than that in the blood [54,55]. Thus, it is possible that chronic and frequent intake of high-dosage (>100 mg/day) capsaicin may lead to significant capsaicin partitioning into lipid membranes and trigger cardiac arrhythmias, especially in patients with comorbid ischemic heart diseases.

4. Materials and Methods

Male New Zealand white rabbits (ca. 2–2.5 kg) were anesthetized by sodium pentobarbitone (40 mg/kg) injection into a marginal ear vein, and following anesthesia, the animal was killed by the removal of the heart. This study was carried out in accordance with the recommendations in the Guide for the Care and Use of Laboratory Animals of the National Institutes of Health and approved by the Animal Care Committee of Bogomoletz Institute of Physiology of the National Academy of Science of Ukraine (approval code: 345/5.7WK). Ventricular myocytes were isolated according to minor modifications of the method described earlier [56,57]. Briefly, the hearts were retrogradely mounted and perfused according to the Langendorff method at a constant flow of 10 mL g heart^{-1} min^{-1} and at 37 °C with a cell isolation solution containing (mM): 130 NaCl, 5.4 KCl, 1.4 $MgCl_2$, 0.75 $CaCl_2$, 0.4 NaH_2PO_4, 5 HEPES, 10 glucose, 20 taurine, and 10 creatine set to pH 7.3 with NaOH. After the stabilization of the heart contractions, perfusion was continued for 4 min with Ca^{2+}-free isolation solution containing 0.1 mM EGTA, and then for 6 min with cell isolation solution containing 0.05 mM Ca^{2+}-, 0.8 mg/mL collagenase (type 1; Worthington Biochemical Corp, USA) and 0.075 mg/mL protease (type X1 V; Sigma, Taufkirchen, Germany). Following enzyme treatment, the heart was removed from the Langendorff perfusion system, and the ventricles were excised, minced, and gently shaken in a collagenase-containing isolation solution supplemented with 1 % BSA. The cells were filtered from this solution at 4 min intervals and resuspended in an isolation solution containing 0.75 mM Ca^{2+}. The shaking and filtration process was repeated up to five times.

4.1. Whole Cell Patch-Clamp Technique

Myocytes were dispersed and allowed to settle for at least one hour at room temperature (22–24 °C) prior to their use. The measurements were performed only in quiescent myocytes displaying normal morphology and clear striated appearance. The whole-cell patch-clamp technique was used to evaluate individual ionic currents using an Axopatch 200B amplifier (Molecular Devices, Sunnyvale, CA, USA) linked to an A/D interface (Digidata 1322; Molecular Devices). The analog signal was filtered using a four-pole Bessel filter with a bandwidth of 5 kHz and digitized at a sampling rate of 10 kHz under software control (PClamp 10.6.2.2, Molecular Devices, Sunnyvale, CA, USA). Heat-polished borosilicate glass pipettes (World Precision Instruments, Sarasota, FL, USA) with a tip resistance of 1 to 2 MΩ were used to establish GΩ seals and continuity with the intracellular medium. The cell capacitance (C_m) was calculated by integrating the area under an uncompensated capacity transient elicited by a 10-mV depolarizing pulse from a holding potential of −80 mV. The total series resistance (R_s) between the pipette interior and the cell membrane in the whole-cell configuration was calculated from the estimates of C_m (172 ± 14 pF, n = 247 from 36 rabbits) and the time constant (τ_c) of the capacitative current decay from the equation $\tau_c = R_s \times C_m$. The mean R_s for the pathway between the pipette and the cell membrane after the rupture of the membrane seal were calculated to be 3.87 ± 0.32 MΩ (n = 247). After the establishment of the whole-cell configuration and the measurement of C_m, the R_s were

compensated to > 60%. The junction potentials under our conditions were approximately −3 mV and were not corrected.

The control perfusate was a modified Tyrode solution containing (in mM): 137 NaCl, 5.4 KCl, 1 $MgCl_2$, 2 $CaCl_2$, 10 HEPES, 10 glucose; titrated with NaOH to pH 7.4. Extracellular solution for recordings of Na^+ currents consisted of (in mM): 100 TEACl, 40 NaCl, 10 glucose, 1 $MgCl_2$, 5 CsCl, 0.1 $CaCl_2$, 10 HEPES [adjusted to pH 7.4 with CsOH; [20]], and 10 μM nifedipine included to suppress L-type Ca^{2+} current. Intracellular solution contained (in mM) 135 CsCl, 5 NaCl, 10, EGTA, 10 HEPES, and 1 MgATP (adjusted to pH 7.25 with CsOH). For the recording of Ca^{2+} currents, the whole-cell bath solution contained (in mM): 95 NaCl, 50 TEACl, 2 $MgCl_2$, 2 $CaCl_2$, 10 HEPES, and 10 glucose (adjusted to pH 7.35 with NaOH). The pipette solution contained (in mM): 140 CsCl, 10 TEACl, 2 $MgCl_2$, 2 HEPES 1 MgATP and 10 EGTA [adjusted to pH 7.25 with CsOH [58]. For recording K^+ currents, the external solution contained (in mM): 132 NaCl, 4 KCl, 1.8 $CaCl_2$, 1.2 $MgCl_2$, 0.2 $BaCl_2$, 10 glucose, 10 HEPES, 5 4-aminopyridine (4-AP), 0.01 nifedipine (pH adjusted to 7.4 with NaOH). The pipette solution for I_K recordings contained (in mM) 120 potassium glutamate, 20 KCl, 2 $MgCl_2$, 10 HEPES, and 5 Mg-ATP; adjusted to pH 7.2 with KOH. When I_{Kr} was recorded, I_{Ks} was inhibited by using 3 μM selective I_{Ks} blocker HMR 1556 (Tocris, Minneapolis, MN, USA). During I_{Ks} measurements, I_{Kr} was blocked by 3 μM dofetilide (Sigma, St. Louis, MO, USA), and the bath solution contained 0.1 μM forskolin (Sigma, St. Louis, MO, USA). Under these conditions, dofetilide (3 μM) and HMR 1556 (3 μM) alone effectively (85–95%) blocked I_{Kr} and I_{Ks}, respectively (n = 4–5). In these recordings, I_{K1}, I_{to}, and $I_{L\text{-}Ca}$ were blocked by 200 μM $BaCl_2$, 5 mM 4-AP, and 10 μM nifedipine, respectively. For recordings of I_{to}, 10 μM nifedipine, 20 μM tetrodotoxin (TTX), and 3 μM dofetilide were included to eliminate $I_{L\text{-}Ca}$, I_{Na}, and I_{Kr}, respectively. These blockers alone ($BaCl_2$, 4-AP, TTX, and nifedipine effectively blocked (85–95%; n = 3–4; without leak subtraction) I_{K1}, I_{to}, I_{Na}, and $I_{L\text{-}Ca}$, respectively.

The experiments were performed at room temperature (22–24 °C). The changes of the external solutions and the application of drugs were performed using a multi-line perfusion system with a common outflow connected to the recording chamber. A perfusion rate of 2 mL/min was used routinely in a recording chamber with a volume of 200 μL.

Capsaicin was from Sigma (St. Louis, MO, USA). It was dissolved in 100 % DMSO, and final concentrations were diluted from stock solutions. The stocks were kept at −20 °C until their use. The highest final concentration of DMSO in the extracellular solutions (0.03% v/v) did not affect the amplitudes of the membrane currents investigated in this study. Capsazepine (dissolved in DMSO), other reagents, and chemicals used in our experiments were purchased from Sigma-Aldrich (St. Louis, MO, USA).

4.2. Statistical Analysis

All of the cumulative results are expressed as mean ± SE or SEM as indicated.

Statistical significance among groups was determined using *t*-test, ANOVA, or pairwise comparisons (Mann–Whitney U-Test) followed by Bonferroni Post-hoc analysis. Statistical analysis of the data was performed using Origin 7.0 software (OriginLab Corp., Northampton, MA, USA). $p < 0.05$ was considered statistically significant. The concentration–response parameters were obtained by fitting the data to the logistic equation in Origin 7.0 software,

$$y = E_{max}/(1 + [x/EC_{50}]^n),$$

where x and y are the concentration and response, respectively, E_{max} is the maximal response, EC_{50} is the half-maximal concentration, and n is the slope factor (apparent Hill coefficient).

Author Contributions: Conceptualization, M.O., F.C.H. and D.I.; methodology, D.I., K.-H.S.Y. and W.S.; software, M.O.; validation, M.O., F.C.H. and D.I.; formal analysis, D.I., K.-H.S.Y. and W.S.; investigation, D.I., K.-H.S.Y. and W.S.; resources, M.O. and K.-H.S.Y.; data curation, D.I., K.-H.S.Y. and W.S.; writing—original draft preparation, D.I. and K.-H.S.Y.; writing—review and editing, M.O.,

F.C.H. and D.I.; visualization, D.I. and M.O.; supervision, M.O. and F.C.H.; project administration, M.O.; funding acquisition, M.O. and K.-H.S.Y. All authors have read and agreed to the published version of the manuscript.

Funding: This research received no external funding.

Institutional Review Board Statement: Animal Care Committee of Bogomoletz Institute of Physiology of National Academy of Science of Ukraine (approval code: 345/5.7WK).

Informed Consent Statement: Not applicable.

Data Availability Statement: Data are contained within the article.

Acknowledgments: Authors thank Donald Bers and Jose Puglisi of the University of California, Davis CA for their help and guidance in using LabHEART v5.3 (Davis, CA, USA).

Conflicts of Interest: The authors declare no conflict of interest.

References

1. O'Neill, J.; Brock, C.; Olesen, A.E.; Andresen, T.; Nilsson, M.; Dickenson, A.H. Unravelling the mystery of capsaicin: A tool to understand and treat pain. *Pharmacol. Rev.* **2012**, *64*, 939–971. [CrossRef]
2. Basith, S.; Cui, M.; Hong, S.; Choi, S. Harnessing the Therapeutic Potential of Capsaicin and Its Analogues in Pain and Other Diseases. *Molecules* **2016**, *21*, 966. [CrossRef]
3. Szabados, T.; Gömöri, K.; Pálvölgyi, L.; Görbe, A.; Baczkó, I.; Helyes, Z.; Jancsó, G.; Ferdinandy, P.; Bencsik, P. Capsaicin-Sensitive Sensory Nerves and the TRPV1 Ion Channel in Cardiac Physiology and Pathologies. *Int. J. Mol. Sci.* **2020**, *21*, 4472. [CrossRef]
4. Miller, M.; Koch, S.E.; Veteto, A.; Domeier, T.; Rubinstein, J. Role of Known Transient Receptor Potential Vanilloid Channels in Modulating Cardiac Mechanobiology. *Front. Physiol.* **2021**, *12*, 734113. [CrossRef]
5. Wang, D.H. The vanilloid receptor and hypertension. *Acta Pharmacol. Sin.* **2005**, *26*, 286–294. [CrossRef]
6. Rubino, A.; Burnstock, G. Capsaicin-sensitive sensory-motor neurotransmission in the peripheral control of cardiovascular function. *Cardiovasc. Res.* **1996**, *31*, 467–479. [CrossRef]
7. Firth, A.L.; Remillard, C.V.; Yuan, J.X. TRP channels in hypertension. *Biochim. Biophys. Acta* **2007**, *1772*, 895–906. [CrossRef]
8. Fukuda, N.; Fujiwara, M. Effect of capsaicin on the guinea-pig isolated atrium. *J. Pharm. Pharmacol.* **1969**, *21*, 622–624. [CrossRef]
9. Molnár, J.; György, L.; Unyi, G.; Kenyeres, J. Effect of capsaicin on the isolated ileum and auricle of the guinea pig. *Acta Physiol. Acad. Sci. Hung.* **1969**, *35*, 369–374.
10. Zernig, G.; Holzer, P.; Lembeck, F. A study of the mode and site of action of capsaicin in guinea-pig heart and rat uterus. *Naunyn Schmiedebergs Arch. Pharmacol.* **1984**, *326*, 58–63. [CrossRef] [PubMed]
11. Franco-Cereceda, A.; Lou, Y.P.; Lundberg, J.M. Ruthenium-red inhibits CGRP release by capsaicin and resiniferatoxin but not by ouabain, bradykinin or nicotine in guinea-pig heart: Correlation with effects on cardiac contractility. *Br. J. Pharmacol.* **1991**, *104*, 305–310. [CrossRef]
12. Kobayashi, Y.; Hoshikuma, K.; Nakano, Y.; Yokoo, Y.; Kamiya, T. The positive inotropic and chronotropic effects of evodiamine and rutaecarpine, indoloquinazoline alkaloids isolated from the fruits of Evodia rutaecarpa, on the guinea-pig isolated right atria: Possible involvement of vanilloid receptors. *Planta Med.* **2001**, *67*, 244–248. [CrossRef]
13. Lundberg, J.M.; Hua, Y.; Fredholm, B.B. Capsaicin-induced stimulation of the guinea-pig atrium. Involvement of a novel sensory transmitter or a direct action on myocytes? *Naunyn Schmiedebergs Arch. Pharmacol.* **1984**, *325*, 176–182. [CrossRef]
14. Miyauchi, T.; Ishikawa, T.; Sugishita, Y.; Saito, A.; Goto, K. Involvement of calcitonin gene-related peptide in the positive chronotropic and inotropic effects of piperine and development of cross-tachyphylaxis between piperine and capsaicin in the isolated rat atria. *J. Pharmacol. Exp. Ther.* **1989**, *248*, 816–824.
15. Franco-Cereceda, A.; Lundberg, J.M. Calcitonin gene-related peptide (CGRP) and capsaicin-induced stimulation of heart contractile rate and force. *Naunyn Schmiedebergs Arch. Pharmacol.* **1985**, *331*, 146–151. [CrossRef]
16. Takaki, M.; Akashi, T.; Ishioka, K.; Kikuta, A.; Matsubara, H.; Yasuhara, S.; Fujii, W.; Suga, H. Effects of capsaicin on mechanoenergetics of excised cross-circulated canine left ventricle and coronary artery. *J. Mol. Cell Cardiol.* **1994**, *26*, 1227–1239. [CrossRef]
17. Yamato, T.; Aomine, M.; Ikeda, M.; Noto, H.; Ohta, C. Inhibition of contractile tension by capsaicin in isolated rat papillary muscle. *Gen. Pharmacol.* **1996**, *27*, 129–132. [CrossRef]
18. Franco-Cereceda, A.; Lundberg, J.M. Actions of calcitonin gene-related peptide and tachykinins in relation to the contractile effects of capsaicin in the guinea-pig and rat heart in vitro. *Naunyn Schmiedebergs Arch. Pharmacol.* **1988**, *337*, 649–655. [CrossRef]
19. Franco-Cereceda, A.; Lundberg, J.M.; Saria, A.; Schreibmayer, W.; Tritthart, H.A. Calcitonin gene-related peptide: Release by capsaicin and prolongation of the action potential in the guinea-pig heart. *Acta Physiol. Scand.* **1988**, *132*, 181–190. [CrossRef]
20. Kury, L.T.A.; Voitychuk, O.I.; Yang, K.H.; Thayyullathil, F.T.; Doroshenko, P.; Ramez, A.M.; Shuba, Y.M.; Galadari, S.; Howarth, F.C.; Oz, M. Effects of the endogenous cannabinoid anandamide on voltage-dependent sodium and calcium channels in rat ventricular myocytes. *Br. J. Pharmacol.* **2014**, *171*, 3485–3498. [CrossRef]

21. Sanguinetti, M.C.; Jurkiewicz, N.K. Two components of cardiac delayed rectifier K^+ current. Differential sensitivity to block by class III antiarrhythmic agents. *J. Gen. Physiol.* **1990**, *96*, 195–215. [CrossRef]
22. Mitcheson, J.S.; Sanguinetti, M.C. Biophysical properties and molecular basis of cardiac rapid and slow delayed rectifier potassium channels. *Cell Physiol. Biochem.* **1999**, *9*, 201–216. [CrossRef]
23. Castle, N.A. Differential inhibition of potassium currents in rat ventricular myocytes by capsaicin. *Cardiovasc. Res.* **1992**, *26*, 1137–1144. [CrossRef]
24. Wu, S.N.; Chen, I.J.; Lo, Y.C.; Yu, H.S. The characteristics in the inhibitory effects of capsaicin on voltage-dependent K^+ currents in rat atrial myocytes. *Environ. Toxicol. Pharmacol.* **1996**, *2*, 39–47. [CrossRef]
25. Xing, J.; Ma, J.; Zhang, P.; Fan, X. Block effect of capsaicin on hERG potassium currents is enhanced by S6 mutation at Y652. *Eur. J. Pharmacol.* **2010**, *630*, 1–9. [CrossRef]
26. Milesi, V.; Rebolledo, A.; Alvis, A.G.; Raingo, J.; de Gende, A.O.G. Voltage-activated sodium current is inhibited by capsaicin in rat atrial myocytes. *Biochem. Biophys. Res. Commun.* **2001**, *282*, 965–970. [CrossRef]
27. Li, Q.; Cheng, Y.P.; He, R.R. Electrophysiological effects of capsaicin on guinea pig papillary muscles. *Sheng Li Xue Bao* **2003**, *55*, 511–515.
28. Cowan, L.M.; Strege, P.R.; Rusinova, R.; Andersen, O.S.; Farrugia, G.; Beyder, A. Capsaicin as an amphipathic modulator of Na (V) 1.5 mechanosensitivity. *Channels* **2022**, *16*, 9–26. [CrossRef]
29. Li, Q.; Wu, Y.M.; He, R.R. Electrophysiological effects of capsaicin on spontaneous activity of rabbit atrioventricular node cells. *Sheng Li Xue Bao* **2004**, *56*, 248–252.
30. Cheng, Y.P.; Wang, Y.H.; Cheng, L.P.; He, R.R. Electrophysiologic effects of capsaicin on pacemaker cells in sinoatrial nodes of rabbits. *Acta Pharmacol. Sin.* **2003**, *24*, 826–830.
31. Puglisi, J.L.; Bers, D.M. LabHEART: An interactive computer model of rabbit ventricular myocyte ion channels and Ca transport. *Am. J. Physiol. Cell Physiol.* **2001**, *281*, C2049–C2060. [CrossRef]
32. D'Alonzo, A.J.; Grover, G.J.; Darbenzio, R.B.; Hess, T.A.; Sleph, P.G.; Dzwonczyk, S.; Zhu, J.L.; Sewter, J.C. In vitro effects of capsaicin: Antiarrhythmic and antiischemic activity. *Eur. J. Pharmacol.* **1995**, *272*, 269–278. [CrossRef]
33. Arnar, D.O.; Cai, J.J.; Lee, H.C.; Martins, J.B. Electrophysiologic effects of civamide (zucapsaicin) on canine cardiac tissue in vivo and in vitro. *J. Cardiovasc. Pharmacol.* **1998**, *32*, 875–883. [CrossRef]
34. Dvorakova, M.; Kummer, W. Transient expression of vanilloid receptor subtype 1 in rat cardiomyocytes during development. *Histochem. Cell Biol.* **2001**, *116*, 223–225. [CrossRef]
35. Hong, J.; Lisco, A.M.; Rudebush, T.L.; Yu, L.; Gao, L.; Kitzerow, O.; Zucker, I.H.; Wang, H.J. Identification of Cardiac Expression Pattern of Transient Receptor Potential Vanilloid Type 1 (TRPV1) Receptor using a Transgenic Reporter Mouse Model. *Neurosci. Lett.* **2020**, *737*, 135320. [CrossRef]
36. Hoebart, C.; Rojas-Galvan, N.S.; Ciotu, C.I.; Aykac, I.; Reissig, L.F.; Weninger, W.J.; Kiss, A.; Podesser, B.K.; Fischer, M.J.M.; Heber, S. No functional TRPA1 in cardiomyocytes. *Acta Physiol.* **2021**, *232*, e13659. [CrossRef]
37. Qi, Y.; Qi, Z.; Li, Z.; Wong, C.K.; So, C.; Lo, I.C.; Huang, Y.; Yao, X.; Tsang, S.Y. Role of TRPV1 in the Differentiation of Mouse Embryonic Stem Cells into Cardiomyocytes. *PLoS ONE* **2015**, *10*, e0133211. [CrossRef]
38. Kury, L.T.A.; Yang, K.H.; Thayyullathil, F.T.; Rajesh, M.; Ali, R.M.; Shuba, Y.M.; Howarth, F.C.; Galadari, S.; Oz, M. Effects of endogenous cannabinoid anandamide on cardiac Na^+/Ca^{2+} exchanger. *Cell Calcium* **2014**, *55*, 231–237. [CrossRef]
39. Melck, D.; Bisogno, T.; De Petrocellis, L.; Chuang, H.; Julius, D.; Bifulco, M.; Di Marzo, V. Unsaturated long-chain N-acyl-vanillyl-amides (N-AVAMs): Vanilloid receptor ligands that inhibit anandamide-facilitated transport and bind to CB1 cannabinoid receptors. *Biochem. Biophys. Res. Commun.* **1999**, *262*, 275–284. [CrossRef]
40. Ingólfsson, H.I.; Thakur, P.; Herold, K.F.; Hobart, E.A.; Ramsey, N.B.; Periole, X.; de Jong, D.H.; Zwama, M.; Yilmaz, D.; Hall, K.; et al. Phytochemicals perturb membranes and promiscuously alter protein function. *ACS Chem. Biol.* **2014**, *9*, 1788–1798. [CrossRef]
41. Greisen, P., Jr.; Lum, K.; Ashrafuzzaman, M.; Greathouse, D.V.; Andersen, O.S.; Lundbæk, J.A. Linear rate-equilibrium relations arising from ion channel-bilayer energetic coupling. *Proc. Natl. Acad. Sci. USA* **2011**, *108*, 12717–12722. [CrossRef]
42. Lundbaek, J.A.; Birn, P.; Tape, S.E.; Toombes, G.E.; Søgaard, R.; Koeppe, R.E., 2nd; Gruner, S.M.; Hansen, A.J.; Andersen, O.S. Capsaicin regulates voltage-dependent sodium channels by altering lipid bilayer elasticity. *Mol. Pharmacol.* **2005**, *68*, 680–689. [CrossRef]
43. Efimova, S.S.; Zakharova, A.A.; Ostroumova, O.S. Alkaloids Modulate the Functioning of Ion Channels Produced by Antimicrobial Agents via an Influence on the Lipid Host. *Front Cell Dev. Biol.* **2020**, *8*, 537. [CrossRef]
44. Efimova, S.S.; Ostroumova, O.S. The Disordering Effect of Plant Metabolites on Model Lipid Membranes of Various Thickness. *Cell Tissue Biol.* **2020**, *14*, 388–397. [CrossRef]
45. Alzaabi, A.H.; Howarth, L.; El Nebrisi, E.; Syed, N.; Susan Yang, K.H.; Howarth, F.C.; Oz, M. Capsaicin inhibits the function of α(7)-nicotinic acetylcholine receptors expressed in Xenopus oocytes and rat hippocampal neurons. *Eur. J. Pharmacol.* **2019**, *857*, 172411. [CrossRef]
46. Nebrisi, E.E.; Prytkova, T.; Lorke, D.E.; Howarth, L.; Alzaabi, A.H.; Yang, K.S.; Howarth, F.C.; Oz, M. Capsaicin Is a Negative Allosteric Modulator of the 5-HT(3) Receptor. *Front. Pharmacol.* **2020**, *11*, 1274. [CrossRef]
47. Oz, M.; Ravindran, A.; Diaz-Ruiz, O.; Zhang, L.; Morales, M. The endogenous cannabinoid anandamide inhibits alpha7 nicotinic acetylcholine receptor-mediated responses in Xenopus oocytes. *J. Pharmacol. Exp. Ther.* **2003**, *306*, 1003–1010. [CrossRef]

48. Oz, M.; Tchugunova, Y.; Dinc, M. Differential effects of endogenous and synthetic cannabinoids on voltage-dependent calcium fluxes in rabbit T-tubule membranes: Comparison with fatty acids. *Eur. J. Pharmacol.* **2004**, *502*, 47–58. [CrossRef]
49. Spivak, C.E.; Lupica, C.R.; Oz, M. The endocannabinoid anandamide inhibits the function of alpha4beta2 nicotinic acetylcholine receptors. *Mol. Pharmacol.* **2007**, *72*, 1024–1032. [CrossRef]
50. Zhang, L.; Oz, M.; Stewart, R.R.; Peoples, R.W.; Weight, F.F. Volatile general anaesthetic actions on recombinant nACh alpha 7, 5-HT3 and chimeric nACh alpha 7-5-HT3 receptors expressed in Xenopus oocytes. *Br. J. Pharmacol.* **1997**, *120*, 353–355. [CrossRef]
51. Jackson, S.N.; Singhal, S.K.; Woods, A.S.; Morales, M.; Shippenberg, T.; Zhang, L.; Oz, M. Volatile anesthetics and endogenous cannabinoid anandamide have additive and independent inhibitory effects on alpha (7) -nicotinic acetylcholine receptor-mediated responses in Xenopus oocytes. *Eur. J. Pharmacol.* **2008**, *582*, 42–51. [CrossRef]
52. Oz, M.; Zhang, L.; Spivak, C.E. Direct noncompetitive inhibition of 5-HT (3) receptor-mediated responses by forskolin and steroids. *Arch. Biochem. Biophys.* **2002**, *404*, 293–301. [CrossRef]
53. Rollyson, W.D.; Stover, C.A.; Brown, K.C.; Perry, H.E.; Stevenson, C.D.; McNees, C.A.; Ball, J.G.; Valentovic, M.A.; Dasgupta, P. Bioavailability of capsaicin and its implications for drug delivery. *J. Control. Release* **2014**, *196*, 96–105. [CrossRef]
54. Saria, A.; Skofitsch, G.; Lembeck, F. Distribution of capsaicin in rat tissues after systemic administration. *J. Pharm. Pharmacol.* **1982**, *34*, 273–275. [CrossRef]
55. Donnerer, J.; Amann, R.; Schuligoi, R.; Lembeck, F. Absorption and metabolism of capsaicinoids following intragastric administration in rats. *Naunyn Schmiedebergs Arch. Pharmacol.* **1990**, *342*, 357–361. [CrossRef]
56. Kury, L.T.A.; Voitychuk, O.I.; Ali, R.M.; Galadari, S.; Yang, K.H.; Howarth, F.C.; Shuba, Y.M.; Oz, M. Effects of endogenous cannabinoid anandamide on excitation-contraction coupling in rat ventricular myocytes. *Cell Calcium* **2014**, *55*, 104–118. [CrossRef]
57. Ali, R.M.; Kury, L.T.A.; Yang, K.H.; Qureshi, A.; Rajesh, M.; Galadari, S.; Shuba, Y.M.; Howarth, F.C.; Oz, M. Effects of cannabidiol on contractions and calcium signaling in rat ventricular myocytes. *Cell Calcium* **2015**, *57*, 290–299. [CrossRef]
58. Isaev, D.; Shabbir, W.; Dinc, E.Y.; Lorke, D.E.; Petroianu, G.; Oz, M. Cannabidiol Inhibits Multiple Ion Channels in Rabbit Ventricular Cardiomyocytes. *Front. Pharmacol.* **2022**, *13*, 821758. [CrossRef]